

# Simulated Analysis Ti-6Al-4V Plate and Screw as Transverse Diaphyseal Fracture Implant for Ulna Bone

*by Prihartini Widiyanti*

---

**Submission date:** 19-May-2023 11:54AM (UTC+0800)

**Submission ID:** 2096779316

**File name:** 2022\_-\_JBBBE\_Simulated\_Ti6Al\_4V\_Plate\_and\_Screw.pdf (1.69M)

**Word count:** 5459

**Character count:** 28492

## Simulated Analysis Ti-6Al-4V Plate and Screw as Transverse Diaphyseal Fracture Implant for Ulna Bone

Mustika Ainun Sabrina<sup>1,a</sup>, Sonia Adilina Hartati<sup>1,b</sup>, Talitha Asmaria<sup>2,c\*</sup>,  
 Prihartini Widiyanti<sup>1,d</sup>, Muhammad Satrio Utomo<sup>2,e</sup>, Fendy Rokhmanto<sup>2,f</sup>  
 and Ika Kartika<sup>1,g</sup>

<sup>1</sup>Biomedical Engineering Study Program, Department of Physics, Faculty of Science and Technology, Airlangga University, Surabaya, Indonesia

<sup>2</sup>Research Center for Metallurgy and Materials, Indonesian Institute of Sciences, Puspiptek Area, South Tangerang, Indonesia

<sup>a</sup>mustika.ainun.sabrina-2018@fst.unair.ac.id, <sup>b</sup>sonia.adilina.hartati-2018@fst.unair.ac.id,  
<sup>c</sup>talitha.asmaria@lipi.go.id, <sup>d</sup>pwidiyanti@fst.unair.ac.id, <sup>e</sup>muha209@lipi.go.id, <sup>f</sup>fend001@lipi.go.id,  
<sup>g</sup>ikak001@lipi.go.id

Corresponding author: talitha.asmaria@lipi.go.id

**Keywords:** Ulnar bone, Bone implant, Transverse diaphyseal fracture, Ti6Al4V

**Abstract.** Transverse diaphyseal fracture is one of the most common fractures caused by accidents. The fracture treatment needs surgery to apply the fixations that matched the bone geometry. This paper aims to reverse engineering of a published bone plate and screw criteria into a three-dimensional (3D) model and analyze them using the finite element method (FEM) in several factors, the bone, the plate, the screw, the unification of plate and screw, and combination all components. This paper conducts two main activities of designing plate and screw based on literature for ulna bone implant and running the FEM to achieve the von Misses stress in the plate, screw, and bone by placing load and constrained area based on the actual use of the implant in the patient. The maximum number in von Misses stress are 5.01855 MPa for bone only, 0.00918 MPa for plate only, 193.304 MPa for screws only, 6.28160 MPa for the assembly screws and a plate, and 761.07 MPa for all unification. All simulation results meet the expectation that the bone analysis is less than the compressive strength of the ulnar bone. Moreover, when applied to the bone, the plate and screw analysis and the assembly also demonstrate a lower number than the yield strength of the properties of the Ti6Al4V materials. All this biomechanical assessment confirms that designs could withstand ulnar bone's ultimate flexural load and pressure. The finite element analysis (FEA) on the proposed recreated dimension on ulnar plate and screw is expected to accelerate the rehabilitation process of radius ulnar fracture, particularly in the transverse diaphyseal fracture in ulna bone.

### Introduction

Traffic accident is a public health problem worldwide. Based on road traffic injuries data by World Health Organization (WHO) in 2020, more than 1.3 million people are killed every year by traffic accidents. The high number of accidents resulting in fractures indicates that the need for bone implants is increasing. One of the most common fractures caused by accidents is the ulnar radius fracture [1]. Bone forearm fracture also might be caused by cancer or other pathologic bone disorders [2]. The discontinuity on the ulnar radius bone, particularly that makes the open fracture, will issue microorganism contamination that eventually causes infection [3]. The treatment by general hospitals offers a procedure of open reduction internal fixation (ORIF) that using the application of plate and screw in the surgery [4]. The developing countries that still have issues on the prosperity of public healthcare providers will suffer the high import numbers in medical devices, such as plates and screws. For example, Indonesian national health insurance, called as BPJS, burdens and debts are generally due to the unresolved obligations of BPJS participants and the high number of imports of medical devices that reach 92% of the equipment availability throughout Indonesia. The independence of self-producing medical tools, such as plates and screws, will tackle the national

health problem. In the self-producing medical equipment industry, a country should consider many aspects, including the failure in the production process, patient use, and post-application evaluation.

FEA has been widely used to predict component response in forces, environmental conditions, and its failure by analyzing the material properties, geometry, mechanical and thermal loads as the input number that helped engineers predict mechanical engineering, thermal and fluid flows, electromagnetic fields, biomathematics, geomechanics, and business management to medical applications [5]–[7]. In addition to material testing, FEA is further employed to measure biomechanical interactions in body organs such as ligaments and bones because it can measure biomechanics influenced by the geometry and structure of organs given a load [8]. For instance, in pre-surgery cases, FEA determines structural analysis of humerus fracture bone to find out the load at which fracture occurs and predict suitable alternative materials for bone implants [9]. In bone implant, a paper analyzes in planning the twelve three-dimensional (3D) implant models to support the prostheses that can predict the variation in geometry, in particular diameter, length, and splinting factors, single-unit crowns, splinted crowns straight-line, and offset implant configuration, has different effects on the mechanical properties of stress and strain in bone tissue which is can helped engineer to calculate and designing implant with low cost [10]. Using the FEA, another paper reveals that the geometry, such as the diameter in a dental implant, has different effects on gap formation and fatigue failure in micro assessments [11]. In addition, the finite element with nonlinear technique has been successfully comparing the post-market evaluation between bone implants in locking plates and conventional plates [12]. Even the FEA has already helped investigate the biomechanical assessment in several surgeries and implant planning conditions. Still, there is no related information on how the finite element works in the bone material itself.

In case of implant for ulnar bone, previous research already presented the designs of plates using composite materials for transverse diaphyseal fracture implant. The paper claimed that the ideal plate for the ulna bone has a length of 78mm. In general, the lower the ratio of plate length to span length, the lower the stiffness of the entire bone and implant when joined. In addition, the paper also mentioned the ideal plate length is 10 mm with a thickness of 4.5mm. At the same time, the distance between the holes is 9.5mm [13]. However, the disadvantage was they did not mention the specific design for the screw itself that fixes the plates for the ulnar bone and on the other side. Another drawback reveals that composite materials are still not a solution for the bone implant because the mechanical properties and degradation rate result in the bones not being fully recovered [9]. Moreover, slowing the degradation rate, the material thickness increases due to low initial mechanical strength and rapid loss of mechanical properties in the bio environment, increasing the cost and quantity required polymers [14]. In fabrication of implant, material selection and review are necessary prior to manufacturing process.

From the previous searches and characteristics of designing ulnar bone implants, note that the design only focused on plate, materials are complex and expensive, and the mechanical properties do not fit enough. For this reason, this study deals with designing the plate and screw that held on a transverse diaphyseal fracture on ulnar bone with FEA that can analyze the design at low cost. The designs using Ti-6Al-4V because it is highly biocompatible and has good mechanical properties with the bone.

## Materials and Method

The method in this paper starts from three geometrical models of screw, plate implant and ulnar bone that created in Solidworks computer aided design (CAD) software (Dassault Systèmes, Vélizy-Villacoublay, France) and exported to Comsol software (Dassault Systèmes, VélizyVillacoublay, France) for pre- and post-processing.

In geometrical model activities, we designed plate and screws are based on literature for ulna bone implants. The literature mentioned that the ideal plate has a cross-section 78 mm long flat plate with a width from 9 mm to 12 mm (with the increments of 1 mm) and a thickness from 3.35 mm to 5 mm (with the increments of 0.5mm) [13]. Figure 1 shows the plate design of this study. In this work, we designed the plate with a length of 78 mm, a thickness of 5 mm (with 0.5 mm number of tolerance)

and the distance between the center points of the holes is 13 mm. This plate is designed with an inner hole of 3.5 mm (with 0.25mm number of tolerance) and an outer hole of 6 mm (with 0.50 mm number of tolerance) to fitted for the screw head to limit excessive plate movement. Figure 1 shows the plate design of this study. The screw head for the plate hole adjusts in the fitted countersink to limit excessive plate movement.

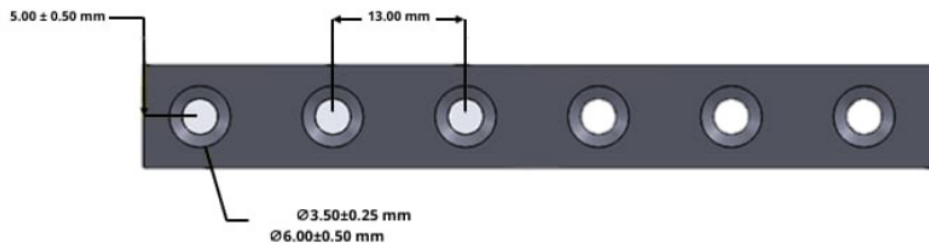


**Figure 1.** Plate design

The bone screw design follows the ISO 5835-1991 standard, using a cortical screw-type method. A literature confirms that the invention is suitable for use as an implant in the fixation of small fragments. Based on the International Organization for Standardization (ISO) 5835:1991 about the ideal screw design is utilizing a 3.5 mm thread diameter with a core diameter of 2.4 mm, a screw head diameter of 6 mm, and a pitch width of 1.25 mm. Another one explains that the anteroposterior diameter of the ulna bone is in the range of 8.5-18.7 mm, with an average of 14.1 mm [15]. By this literature, the screw was designed with a length of 14.8 mm, which measured from the screw neck to the tip, so the overall size of the screw from head to the tip is 18.6 mm. Figure 2 shows the screw configuration for the proposed implant. The screw length that enters the bone will be the overall screw length minus the plate thickness. Here, we can calculate that the screw part that joins to the bone is about 10 mm. It is more than half of the average ulna bone diameter.

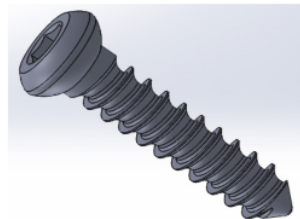


**Figure 2.** Screw design

In the biomechanical study of bone and implant, FEA performs complex computations commonly used to simulate materials to determine their characterization [16]. This method uses a general numerical approach, namely differential equations, to solve physical problems by determining stress and strain values in material elements. Furthermore, FEA stress that acts perpendicular to the work surface. Stress, symbolized by sigma ( $\sigma$ ), occurs due to axial and bending forces. In computational testing, the stress test is generally symbolized by von Mises stress (VMS). VMS is a failure test of material when viewed from the distortion energy per volume greater than the principal stress value in the material [17].

In this work, the implant and screw design models were converted into a .stp file and computed in Comsol software. The load and constrained area were loaded based on the actual use of the implant in the patient as well as a consideration of meshing type based on the ability to compute the software. The load and force number exercised in this study is the ultimate flexural load in the ulna, which is 466 N [13]. The computational study was run using Ti6Al4V material, provided by the software. Table 1 shows the Ti6Al4V used in this study [18]–[20]. TiAl6V4 is one of the most commonly used

titanium alloys. It has very good biomechanical characteristics and good weldability usually used in the medical field. The material has high biocompatibility, which is lightweight, and has easy mass production [21]. This lightweight metal alloy also has high strength number with high corrosion resistance that suitable for medical purpose.

**Table 1.** Mechanical Properties of Ti-6Al-4V [18]–[20]

Parameter	Value
Density (kg/m <sup>3</sup> )	4428.78
Tensile Strength (GPa)	1.05
Yield Strength (GPa)	0.827
Elastic Modulus (GPa)	104.8
Shear Modulus (GPa)	41.02
Poisson's Ratio	0.31

## Results

FEA in this study was run in five conditions, those were on the ulnar bone with hydroxyapatite material; bone plate with Ti6Al4V; screw with Ti6Al4V; the combination of bone plate and screw using Ti6Al4V; and a unify the bone and plate and screw. The selection of meshing features is based on the ability of the software to compute, whereas the consideration of load placement is based on the area that can have more contact with the human bone [18]. The utilized force number in this study is 466 N as the number of the ultimate flexural load of ulnar bone [13]. First of all, the ulnar bone simulation itself use hydroxyapatite material. It is adapted to the biomechanical conditions and properties of cortical bone. The placement of load in the area that will contact with the plate and all holes; the rest area was constrained. The mesh convergence is using normal mesh treatment with has 4069 domain elements and 2560 boundary elements. By this simulation, it achieves 5.08155 MPa as the maximum VMS. Figure 3 show the maximum VMS as the red color places in the area that will be in contact with the implant tools.

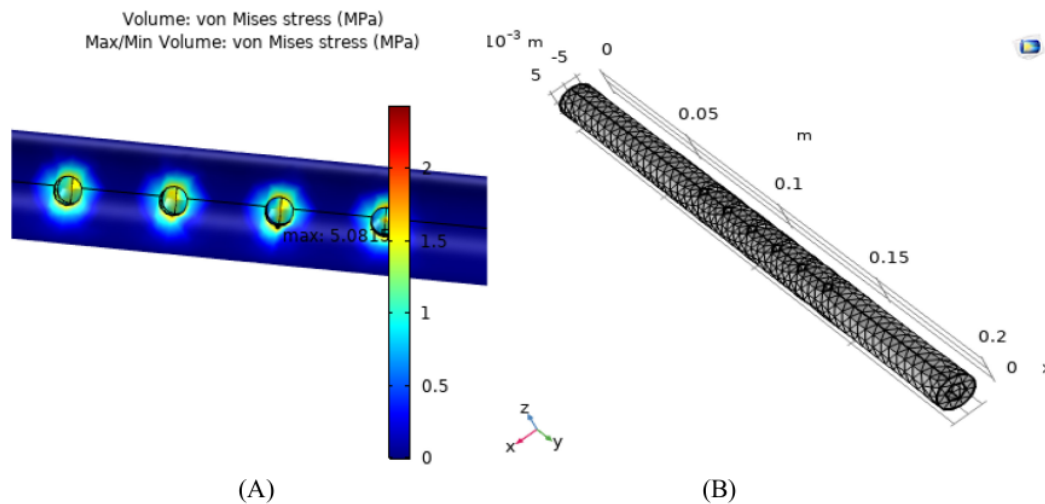


**Figure 3.** Von Mises stress (A) and its meshing design (B) on the ulna bone.

Secondly, in the experiment of bone plate using Ti6Al4V material selection, the plate was meshed extremely fine by having 75863 domain elements, 11514 boundary elements, and 1230 edge elements. The constraints were placed in the area that will in touch with the bone, whereas the load was placed in the rest of the area, consist of the area that has holes for screw and 5 other sides. From the FEA simulation, the maximum VMS is 0.00918 MPa, located at the bottom of the bone plate,

which is the cross-section when the plate is pressured to the -z-axis. The minimum pressure is 0.00002 MPa, located on the inside of the screw hole. Figure 4 indicates the maximum and minimum VMS on the bone plate and its meshing divergence. In FEA computation of screw, the load number was given on the whole head surface of the screw and the screw tip, whereas on the entire screw rod that has threads were constrained. The screw was meshed using a feature of finer with created 75863 domain elements, 11514 boundary elements, and 1230 edge elements. The FEA produces 193,304 MPa as the maximum VMS value. Figure 5 shows the critical point of the screw is in the bottom of head screw. This area also gets more pressure when applied with the bone plate.

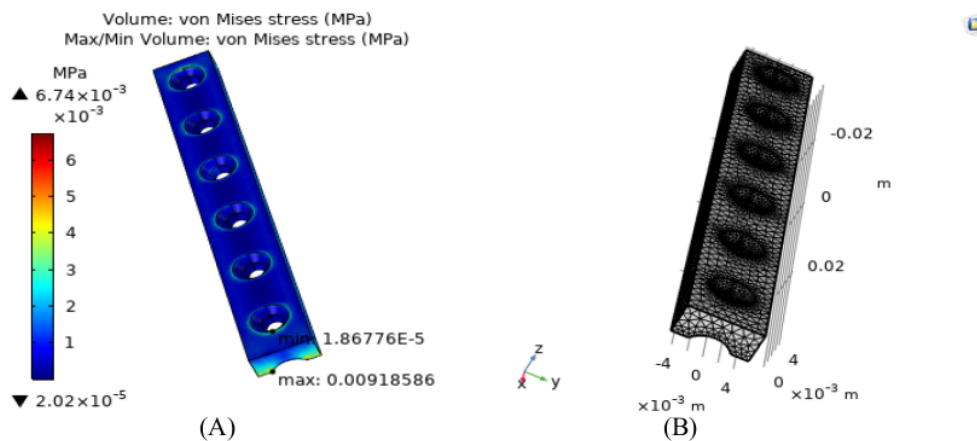


Figure 4. Von Misses stress (A) and its meshing design (B) on the ulna bone.

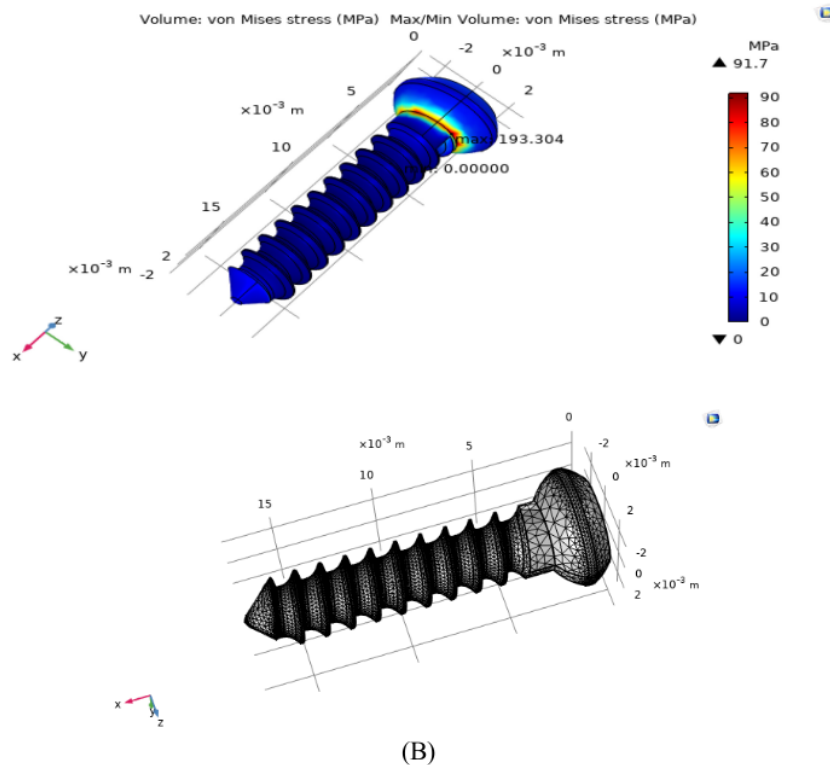
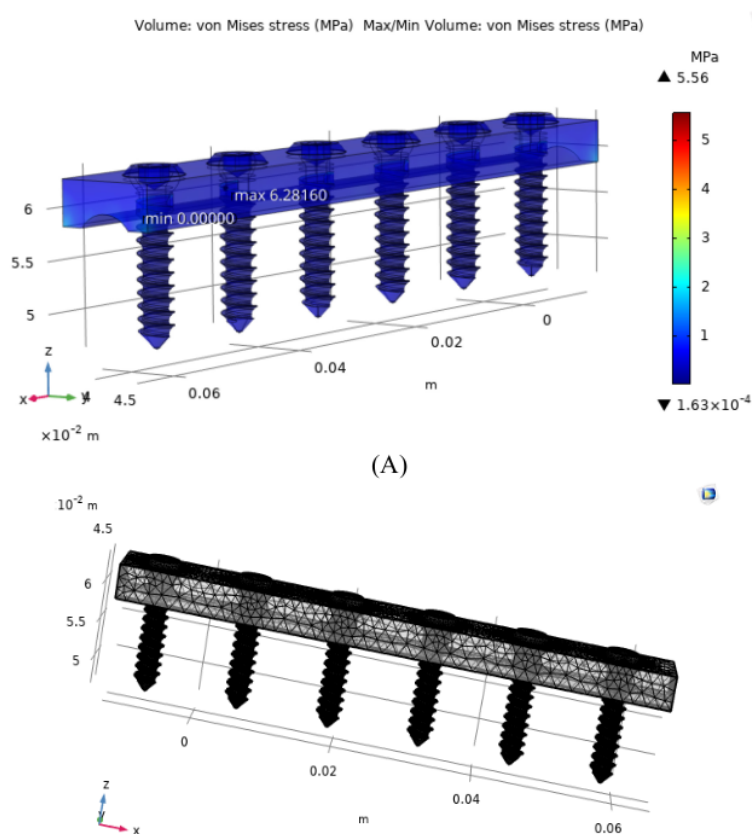
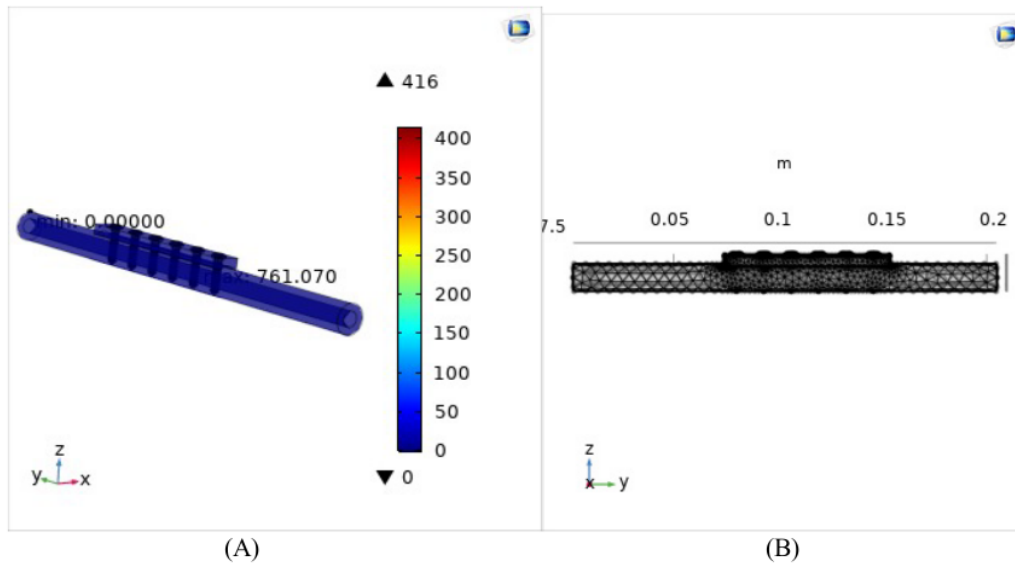


Figure 5. Von Misses stress (A) and its meshing design (B) on the proposed screw

Lastly, in two experiments of metal combination, plate and screws, and a unify of bone and the implant were using different type of mesh, those were finer and coarse, respectively. In the one set of a bone plate and six screws using Ti6Al4V, the mesh divergence created 206888 domain elements, 59823 boundary elements, and 14915 edge elements. Placement of all load were located in the whole head screw, one side of plate that contacted directly with the screw and the tip screw. The constrained areas were place in five sides of plate that not in contact with the screw and in the screw rod that contains threads. The FEA produces a maximum VMS number of 6.28160 MPa; while the minimum value is 0 MPa. Figure 6 shows that almost all configuration has blue color. The area that has a red color is limited and placed at the neck screw area. Unlike the unify of plate and the six screws, the combination with ulnar bone was using coarse as a type of mesh divergence. The model was meshed and generates 174092 domain elements, 58030 boundary elements, and 14290 edge elements. Placement of the loads were in the all sides of plate and screw; whereas the ulnar bone area was constrained. The FEA computation presents that the maximum value VMS is 761.07 MPa, and the minimum value generated is 0 MPa. Figure 7 also shows that most all area has blue color, however the critical point of red colors are in meeting points between plate and screw as well as with the ulnar bone. Table 2 summarizes all VMS values in five experiments in this study.



**Figure 6.** Von Misses stress (A) and its meshing design (B) on the proposed bone plate and screw



**Figure 7.** Von Misses stress (A) and its meshing design (B) on the proposed bone plate and screw attached to the ulna bone

**Table 2.** Von Misses Stress Values in All Designs

Design Type	Mesh Type	Von Misses Stress (Mpa)	
		Max	Min
<b>Ulnar Bone (Hydroxyapatite)</b>	Normal	5.08155	0
<b>Bone Plate (Ti6Al4V)</b>	Extremely Fine	0.00918	0.00002
<b>Bone Screw (Ti6Al4V)</b>	Finer	193.304	0
<b>Plate combined with 6 Screws (Ti6Al4V)</b>	Finer	6.2816	0
<b>Plate with 6 Screws intact on ulnar bone</b>	Coarse	761.07	0

## Discussion

Based on five experiments that produce VMS values in all designs, the VMS on ulnar bone has the maximum value of 5.08155 MPa. Table 3 shows the mechanical properties of the ulna bone. Compared to the compressive strength of the ulna bone, which is 78.19 MPa, the VMS result on ulnar bone indicates that the ulna bone is strong enough with a given load to the screws and plates, which will later be implanted in the bone [22]. This paragraph will only discuss the first result of bone's VMS. Bone is a viscoelastic material, and its properties depend on the rate of strain. The ulna bone is the stabilizer bone in the forearm, located medially, and is the long bone of the two forearms bones. The ulna is the medial bone of the antebrachium. The proximal end of the ulna is large and called the olecranon, and this structure forms the protrusion of the elbow. The biomechanical character of bone usually determines the weighting of bone strength. Bone strength depends on mineral content, density, elastic modulus, size, shape, age, and sex [23]. Transverse diaphysis fracture of the ulna is a fracture that is transverse to the bone and results in angulation or direct trauma. In fracture rehabilitation using implants, the consideration of selecting the implant must be adjusted to the fracture examination of the patient and factors such as fracture healing, number of fractures, fracture line fracture, size, and activeness of the patient [24]. Other factors in the rehabilitation of bone



fractures are proper surgery, minimal dissection, protection of soft tissue and bone in the area, anatomical or indirect reduction, adequate stabilization, selection of appropriate materials and applications, and appropriate postoperative care [25]. Bone implants can be natural or synthetic materials that have the purpose of bone reconstruction or as other implant protections [26]. Bone consists mostly of hydroxyapatite (HA) with the chemical formula  $(Ca_{10}(PO_4)_6(OH)_2)$  is 69% of the composition of bone, tooth enamel, and inorganic components in dentin [27]. HA is a hydroxylated calcium phosphate salt with a high degree of hardness, and the main component has a similar chemical composition to inorganic substances in bones and teeth [28]. HA has biological properties such as excellent biocompatibility and is osteoconductive. Due to its bioactivity and resorption properties, HA allows direct bonding to bone tissue [29]. From the ulnar bone simulation design with hydroxyapatite material, the obtained results show its biomechanical conditions that can be adapted to the properties of the ulna bone.

**Table 3. Mechanical Properties of Ulna Bone [22]**

Test Type	Mechanical Property	Mean ( $\pm$ SD) Ulna Bone
<b>Bending Test</b>	Bending Strength (MPa)	135.16 (30.43)
	Bending Modulus (GPa)	4.49 (1.14)
	Bending Stiffness (kN/mm)	1.11 (0.06)
<b>Compression Test</b>	Maximum Compression Force (kN)	0.0 (2.28)
	Compressive Strength (MPa)	78.19 (1.16)
	Elastic Modulus (GPa)	3.05 (1.03)
	Compression Stiffness(kN/mm)	11.64(3.01)
<b>Fracture Toughness Test</b>	Fracture fracture force (kN) in notched samples under 3 point bending test	0.05(0.17)
	Fracture Toughness (MPa/m)	15.76(5.61)

One of many standards in finite element computation, particularly to find the VMS as the main parameter, is when the VMS results should be less than the yield strength of the used material [19,30]. The maximum stress value generated in the design has a smaller value than the yield strength value of the Ti6Al4V material. It reveals that the plate and screw design have good enough strength to be not easily cracked when applied to the bone. That is also shown on the plate and screw combined design, which has a VMS number of 6.28160 MPa while the minimum value is 0 MPa. It proves that the ability to withstand the load on the plate and screw is very good because compared to the yield strength value on Ti6Al4V, the combined plate and screws component has a much smaller value. FEA installing a plate with six screws on the ulna bone model to see the strength of the ulna bone. FEA computations present that the maximum value of von Mises stress induced in the simulation is 761.07 MPa, and the minimum value generated is 0 MPa. The resulting value is then compared with the yield strength value of the Ti6Al4V to see if the ulna bone can accept the load or total force applied by the plate and screw without changing. The maximum stress value generated in this design has a value that is smaller than the yield strength of Ti6Al4V materials. It validates that the ulna bone can withstand the load or the total force provided by the plate and screw and does not experience cracks caused by the load.

Several close studies complete the analysis of this work. A complex examination of treatment in the forearm fractures has been done using FEA and comparative clinical assessment on the patient's hand 3D model. A volume computed tomography (CT) data was acquired to build the forearm models and apply 400MPa in several areas on the forearms. The result shows that both biomechanical analysis and clinical study still have advantages of the casting technology in the velcro straps as the patient-specific fixing devices. In another work, a 3D-CT data of a ten-year-old boy suffered from an occult fracture to the elbow after minor trauma. A humerus model was then refined to design a patient-

specific of fixation system within K-wires. The finite element was utilized to analyze the stiffness on all K wire models. A previous finite element study of locking plate for treatment of ulnar head fracture using Ti6Al4V material selections. It has been conducted using a real 3D ulnar model based on CT data patient, investigated using two types of load [31]–[33]. The fixation system can be different and special depending on the fracture case.

This work simulates the FEA for the published and recommended dimension for ulnar bone fracture, particularly the transverse diaphyseal fracture. The only weakness of this study is not using the real model of ulnar bone from a patient data. So far, we have succeeded in conducting five simulations to understand the phenomena on each component and when the implants are applied. The implication of this study is expected to contribute to the new standard of how the FEA conducted in bone-plate simulation, in which the computational study should apply not only for the proposed implant, but also for the applied bone. In the forthcoming development, to accomplish and improve the result to have more precise number and close to the real condition, the experiments can be continued to form the bone based on the CT data patient and perform the bone material simulation in the original bone geometry. In addition, clinical trials will enhance product development in physical functions.

### Summary

Finite element analysis on the ulnar bone, the ulnar bone plate, the matched screws, the set of plate and screws, and the set of ulna bone installed with plate and screw has purposed to accelerate the rehabilitation process of radius ulnar fracture, particularly in the transverse diaphyseal fracture in ulna bone. The experiment was given a load of 466N as ultimate flexural load in the ulna, produce the maximum pressure in von Misses stress format of 5.01855 MPa, 0.00918 MPa, 193,304 MPa, 6.28160 MPa, 761.07 MPa. The von Misses stress maximum number in the ulnar bone is smaller than the compressive strength of the ulna bone. Therefore, it proves that the bone is capable of accepting the given load. Furthermore, the von Misses stress maximum number in the Ti6Al4V components has smaller numbers than the yield strength of the Ti6Al4V properties and indicated that it could withstand the full load of the ulnar bone. In future work, the simulation of 3D bone based on patient data will improve the outcomes.

### Acknowledgement

The publication fee was funded using the national priority research program from Indonesian Endowment Fund for Education (LPDP) number 10/E1/II/PRN/2020.

### References

- [1] Z. Atanelov and T. P. Bentley, “Greenstick Fracture,” *StatPearls*, Aug. 2021, Accessed: Oct. 15, 2021. [Online]. Available: <https://www.ncbi.nlm.nih.gov/books/NBK513279/>
- [2] R. F. Small and A. M. Yaish, “Radius and Ulnar Shaft Fractures,” *Essential Orthopedic Review: Questions and Answers for Senior Medical Students*, pp. 61–62, May 2021, Accessed: Oct. 15, 2021. [Online]. Available: <https://www.ncbi.nlm.nih.gov/books/NBK557681/>
- [3] A. M. (Anne M. Sylvestre, “Fracture management for the small animal practitioner,” p. 282.
- [4] L. KF, L. L, and B. PK, “Outcomes of Distal Ulna Fractures Associated With Operatively Treated Distal Radius Fractures,” *Hand (New York, N.Y.)*, vol. 15, no. 3, pp. 418–421, May 2020, doi: 10.1177/1558944718812134.
- [5] A. K. Devaraj, K. K. v. Acharya, and R. Adhikari, “Experimental and Finite Element Investigations on the Biomechanical Effects of Meniscal Tears in the Knee Joint: A Review,” *Journal of Biomimetics, Biomaterials and Biomedical Engineering*, vol. 50, pp. 1–14, 2021, doi: 10.4028/WWW.SCIENTIFIC.NET/JBBBE.50.1.

- 
- [6] B. Mohammadi, Z. Abdoli, and E. Anbarzadeh, "Investigation of the Effect of Abutment Angle Tolerance on the Stress Created in the Fixture and Screw in Dental Implants Using Finite Element Analysis," *Journal of Biomimetics, Biomaterials and Biomedical Engineering*, vol. 51, pp. 63–76, Jun. 2021, doi: 10.4028/WWW.SCIENTIFIC.NET/JBBBE.51.63.
- [7] A. Rao, "APPLICATIONS OF FINITE ELEMENTS METHOD (FEM) -AN OVERVIEW." Oct. 2012. doi: 10.13140/RG.2.2.36294.42565.
- [8] D. Ruffoni, "Chapter 09798 - 3.10 Finite Element Analysis in Bone Research A Computational Method Relating Structure to Mechanical Function," *Comprehensive Biomaterials II*, vol. 3, 2017, doi: 10.1016/B978-0-12-803581-8.09798-8.
- [9] K. C. Nithin Kumar, N. Griya, A. Shaikh, V. Chaudhry, and S. Chavadaki, "Structural analysis of femur bone to predict the suitable alternative material," *Materials Today: Proceedings*, vol. 26, pp. 364–368, Jan. 2020, doi: 10.1016/J.MATPR.2019.12.031.
- [10] V. E. de S. Batista *et al.*, "Effect of the acrylic occlusal device on the stress distribution in the external hexagon implant in situations of dental tightening. A 3D finite element analysis," *Research, Society and Development*, vol. 10, no. 6, p. e33610615601, May 2021, doi: 10.33448/rsd-v10i6.15601.
- [11] H. Lee, M. Jo, and G. Noh, "Biomechanical effects of dental implant diameter, connection type, and bone density on microgap formation and fatigue failure: A finite element analysis," *Computer Methods and Programs in Biomedicine*, vol. 200, p. 105863, Mar. 2021, doi: 10.1016/J.CMPB.2020.105863.
- [12] M. Miura *et al.*, "Prediction of fracture load and stiffness of the proximal femur by CT-based specimen specific finite element analysis: cadaveric validation study," *BMC Musculoskeletal Disorders 2017 18:1*, vol. 18, no. 1, pp. 1–8, Dec. 2017, doi: 10.1186/S12891-017-1898-1.
- [13] N. D. Chakladar, L. T. Harper, and A. J. Parsons, "Optimisation of composite bone plates for ulnar transverse fractures," *Journal of the Mechanical Behavior of Biomedical Materials*, vol. 57, pp. 334–346, Apr. 2016, doi: 10.1016/J.JMBBM.2016.01.029.
- [14] P. Wan, C. Yuan, L. L. Tan, Q. Li, and K. Yang, "Fabrication and evaluation of bioresorbable PLLA/magnesium and PLLA/magnesium fluoride hybrid composites for orthopedic implants," *Composites Science and Technology*, vol. 98, pp. 36–43, Jun. 2014, doi: 10.1016/J.COMPSCITECH.2014.04.011.
- [15] H. Erdem, "Surgical Importance of Radiographically Aided Morphometry of the Proximal Ulna," *International Journal of Morphology*, vol. 38, no. 2, pp. 299–304, Apr. 2020, doi: 10.4067/S0717-95022020000200299.
- [16] V. Caraveo, S. Lovald, T. Khraishi, V. Caraveo, S. Lovald, and T. Khraishi, "A Study of the Mechanical Characteristics of a Mandibular Parasymphiseal Fracture with Internal Fixation Device Subject to Variable Bite Forces: Finite Element Analysis," *Journal of Biosciences and Medicines*, vol. 9, no. 4, pp. 158–178, Mar. 2021, doi: 10.4236/JBM.2021.94014.
- [17] V. B. Bhandari, *Design of machine element*. McGraw-Hill, 2010.
- [18] D. P. Malau, Y. Whulanza, D. Annur, Y. Prabowo, M. S. Utomo, and M. I. Amal, "Proximal femur prosthesis remodeling and stress evaluation for Indonesian patient," *AIP Conference Proceedings*, vol. 2088, Mar. 2019, doi: 10.1063/1.5095334.
- [19] D. P. Malau *et al.*, "Finite element analysis of porous stemmed hip prosthesis for children," *AIP Conference Proceedings*, vol. 2193, p. 50019, Dec. 2019, doi: 10.1063/1.5139393.
- [20] M. S. Utomo *et al.*, "The effect of patellar groove on mechanical performance of femoral component," *AIP Conference Proceedings*, vol. 2227, p. 20003, May 2020, doi: 10.1063/5.0000927.

- 
- [21] D. Annur, I. Kartika, S. Supriadi, and B. Suharno, "Titanium and titanium based alloy prepared by spark plasma sintering method for biomedical implant applications - A review," *Materials Research Express*, vol. 8, no. 1, Jan. 2021, doi: 10.1088/2053-1591/ABD969.
- [22] D. Singh, A. Rana, S. K. Jhahria, B. Garg, P. M. Pandey, and D. Kalyanasundaram, "Experimental assessment of biomechanical properties in human male elbow bone subjected to bending and compression loads," *Journal of Applied Biomaterials and Functional Materials*, vol. 17, no. 2, Apr. 2019, doi: 10.1177/2280800018793816.
- [23] E. F. Morgan, G. U. Unnikrisnan, and A. I. Hussein, "Bone Mechanical Properties in Healthy and Diseased States," *Annual review of biomedical engineering*, vol. 20, p. 119, Jun. 2018, doi: 10.1146/ANNUREV-BIOENG-062117-121139.
- [24] A. L. Johnson, "Fundamentals of Orthopedic Surgery and Fracture Management - Plate and Screw Fixation," *Small Animal Surgery Textbook*, pp. 1086–1093, 2013.
- [25] T. J. Vet Anim Sci *et al.*, "Turkish Journal of Veterinary and Animal Sciences The treatment of supracondylar and diaphyseal femoral fractures in cats using intramedullary two-way stacked Kirschner wire application", doi: 10.3906/vet-1606-12.
- [26] M. R. Senra and M. de F. V. Marques, "Synthetic Polymeric Materials for Bone Replacement," *Journal of Composites Science 2020, Vol. 4, Page 191*, vol. 4, no. 4, p. 191, Dec. 2020, doi: 10.3390/JCS4040191.
- [27] K. Pajor, L. Pajchel, and J. Kolmas, "Hydroxyapatite and Fluorapatite in Conservative Dentistry and Oral Implantology—A Review," *Materials*, vol. 12, no. 17, 2019, doi: 10.3390/MA12172683.
- [28] F. Coelho *et al.*, "Silk fibroin/hydroxyapatite composite membranes: Production, characterization and toxicity evaluation," *Toxicology in Vitro*, vol. 62, p. 104670, Feb. 2020, doi: 10.1016/J.TIV.2019.104670.
- [29] H. TU, A. DV, and B. M, "Hydroxyapatite Dental Material," *StatPearls*, Jul. 2018, Accessed: Oct. 16, 2021. [Online]. Available: <http://europepmc.org/books/NBK513314>
- [30] D. Annur *et al.*, "Material selection based on finite element method in customized iliac implant," *Materials Science Forum*, vol. 1000 MSF, pp. 82–89, 2020, doi: 10.4028/WWW.SCIENTIFIC.NET/MSF.1000.82.
- [31] Y. Zhang *et al.*, "Finite element analysis of different locking plate fixation methods for the treatment of ulnar head fracture," *Journal of Orthopaedic Surgery and Research 2021 16:1*, vol. 16, no. 1, pp. 1–13, Mar. 2021, doi: 10.1186/S13018-021-02334-4.
- [32] C. Liu, A. Kamara, T. Liu, Y. Yan, and E. Wang, "Mechanical stability study of three techniques used in the fixation of transverse and oblique metaphyseal-diaphyseal junction fractures of the distal humerus in children: a finite element analysis," *Journal of Orthopaedic Surgery and Research 2020 15:1*, vol. 15, no. 1, pp. 1–8, Jan. 2020, doi: 10.1186/S13018-020-1564-4.
- [33] Y. Chen *et al.*, "Application of 3D-Printed Orthopedic Cast for the Treatment of Forearm Fractures: Finite Element Analysis and Comparative Clinical Assessment," *BioMed Research International*, vol. 2020, 2020, doi: 10.1155/2020/9569530.

# Simulated Analysis Ti-6Al-4V Plate and Screw as Transverse Diaphyseal Fracture Implant for Ulna Bone

## ORIGINALITY REPORT

15%

SIMILARITY INDEX

11%

INTERNET SOURCES

13%

PUBLICATIONS

1%

STUDENT PAPERS

## PRIMARY SOURCES

1	<p>Pramestia Nur Safitri, Amelia, Talitha Asmaria, Osmalina Nur Rahma, Ahmad Jabir Rahyussalim, Salsabila Aurellia, Ika Kartika. "Stem Geometry Recommendation for Total Hip Replacement Planning Using Computed Tomography Data Analysis", Journal of Biomimetics, Biomaterials and Biomedical Engineering, 2022</p> <p>Publication</p>	2%
2	<p><a href="http://journal.unesa.ac.id">journal.unesa.ac.id</a></p> <p>Internet Source</p>	2%
3	<p><a href="http://moam.info">moam.info</a></p> <p>Internet Source</p>	1%
4	<p><a href="http://eprints.whiterose.ac.uk">eprints.whiterose.ac.uk</a></p> <p>Internet Source</p>	1%
5	<p><a href="http://ir.unimas.my">ir.unimas.my</a></p> <p>Internet Source</p>	1%
6	<p><a href="http://www.mdpi.com">www.mdpi.com</a></p> <p>Internet Source</p>	1%

7	<a href="http://josr-online.biomedcentral.com">josr-online.biomedcentral.com</a> Internet Source	1 %
8	<a href="http://journals.plos.org">journals.plos.org</a> Internet Source	1 %
9	<p>ALTUNATMAZ, Kemal, KARABAĞLI, Murat, AYDIN KAYA, Didar, GÜZEL, Özlem, ERAVCI YALIN, Ebru, UĞURLU, Ümit, ŞADALAK, Defne Joan and EKİCİ, Himmet. "The treatment of supracondylar and diaphyseal femoral fractures in cats using intramedullary two-way stacked Kirschner wire application", TÜBİTAK, 2017.</p> Publication	1 %
10	<a href="http://ouci.dntb.gov.ua">ouci.dntb.gov.ua</a> Internet Source	1 %
11	<p>Amel Boukhelif, Ali Merdji, Nouredine Della, El Bahri Ould Chikh, Osama Mukdadi, Rajshree Hillstrom. "Numerical Evaluation of Biomechanical Stresses in Dental Bridges Supported by Dental Implants", Journal of Biomimetics, Biomaterials and Biomedical Engineering, 2018</p> Publication	1 %
12	<a href="http://www.docme.ru">www.docme.ru</a> Internet Source	<1 %

- |    |  |      |
|----|--|------|
| 13 | N.D. Chakladar, L.T. Harper, A.J. Parsons. "Optimisation of composite bone plates for ulnar transverse fractures", Journal of the Mechanical Behavior of Biomedical Materials, 2016<br>Publication   | <1 % |
| 14 | <a href="https://dspace.sctimst.ac.in">dspace.sctimst.ac.in</a><br>Internet Source   | <1 % |
| 15 | <a href="https://en.globes.co.il">en.globes.co.il</a><br>Internet Source   | <1 % |
| 16 | Muhammad S. Utomo, Muhammad I. Amal, Sugeng Supriadi, Daniel Malau, Dhyah Annur, Andika W. Pramono. "Design of modular femoral implant based on anthropometry of Eastern Asian", AIP Publishing, 2019<br>Publication                       | <1 % |
| 17 | <a href="https://pubmed.ncbi.nlm.nih.gov">pubmed.ncbi.nlm.nih.gov</a><br>Internet Source   | <1 % |
| 18 | Fernanda Coelho, Mauricio Cavicchioli, Sybele Saska Specian, Eduardo Maffud Cilli et al. "Silk fibroin/hydroxyapatite composite membranes: Production, characterization and toxicity evaluation", Toxicology in Vitro, 2020<br>Publication | <1 % |
| 19 | Ilona Plesa, Petru V. Notingher, Sandra Schlogl, Cristina Stancu et al. "Structural Model for the Estimation of the Equivalent   | <1 % |

Permittivity of Nanodielectrics Based on Polyethylene and Epoxy Resins", IEEE Access, 2021

Publication

---

20

Xiaohong Yin, Qi Li, Yirong Hong, Xiaowen Yu, Xianyan Yang, Zhaonan Bao, Mengfei Yu, Huayong Yang, Zhongru Gou, Bin Zhang.

"Customized reconstruction of alveolar cleft by high mechanically stable bioactive ceramic scaffolds fabricated by digital light processing", Materials & Design, 2022

Publication

---

21

Xuefeng Xiong, Li Li, Hong Li, Peng Zan. "Thermal Stress Analysis for Carbon/Carbon Material Throat Lining Based on Finite Element Analysis", Journal of Physics: Conference Series, 2022

Publication

---

22

[qspace.qu.edu.qa](http://qspace.qu.edu.qa)

Internet Source

---

23

"Proceedings of the 1st International Conference on Electronics, Biomedical Engineering, and Health Informatics", Springer Science and Business Media LLC, 2021

Publication

---

24

Dhyah Annur, Muhammad S. Utomo, Talitha Asmaria, Daniel P. Malau et al. "Material Selection Based on Finite Element Method in

<1 %

<1 %

<1 %

<1 %

<1 %



# Customized Iliac Implant", Materials Science Forum, 2020

Publication

---

25 Said Kebdani, S. Kebdani, M. Dahmane, Z. Azari. "Biomechanical Comparison between Two Models of the Lumbar Intersomatic Fusion Cage Analyzed by the Finite Element Method", Journal of Biomimetics, Biomaterials and Biomedical Engineering, 2017  
Publication

<1 %

---

26 core.ac.uk  
Internet Source

<1 %

---

27 dokumen.pub  
Internet Source

<1 %

---

28 downloads.hindawi.com  
Internet Source

<1 %

---

29 iknow-imeri.fk.ui.ac.id:8080  
Internet Source

<1 %

---

30 www.hindawi.com  
Internet Source

<1 %

---

31 www.scirp.org  
Internet Source

<1 %

---

32 Dilpreet Singh, Bhavuk Garg, Pulak Mohan Pandey, Dinesh Kalyanasundaram. "Design and development of 3D printing assisted microwave sintering of elbow implant with

<1 %

# biomechanical properties similar to human elbow", Rapid Prototyping Journal, 2021

Publication

---

---

Exclude quotes  On

Exclude matches  < 5 words

Exclude bibliography  On

# Simulated Analysis Ti-6Al-4V Plate and Screw as Transverse Diaphyseal Fracture Implant for Ulna Bone

---

GRADEMARK REPORT

---

FINAL GRADE

**/0**

GENERAL COMMENTS

**Instructor**

---

PAGE 1

---

PAGE 2

---

PAGE 3

---

PAGE 4

---

PAGE 5

---

PAGE 6

---

PAGE 7

---

PAGE 8

---

PAGE 9

---

PAGE 10

---

PAGE 11

---